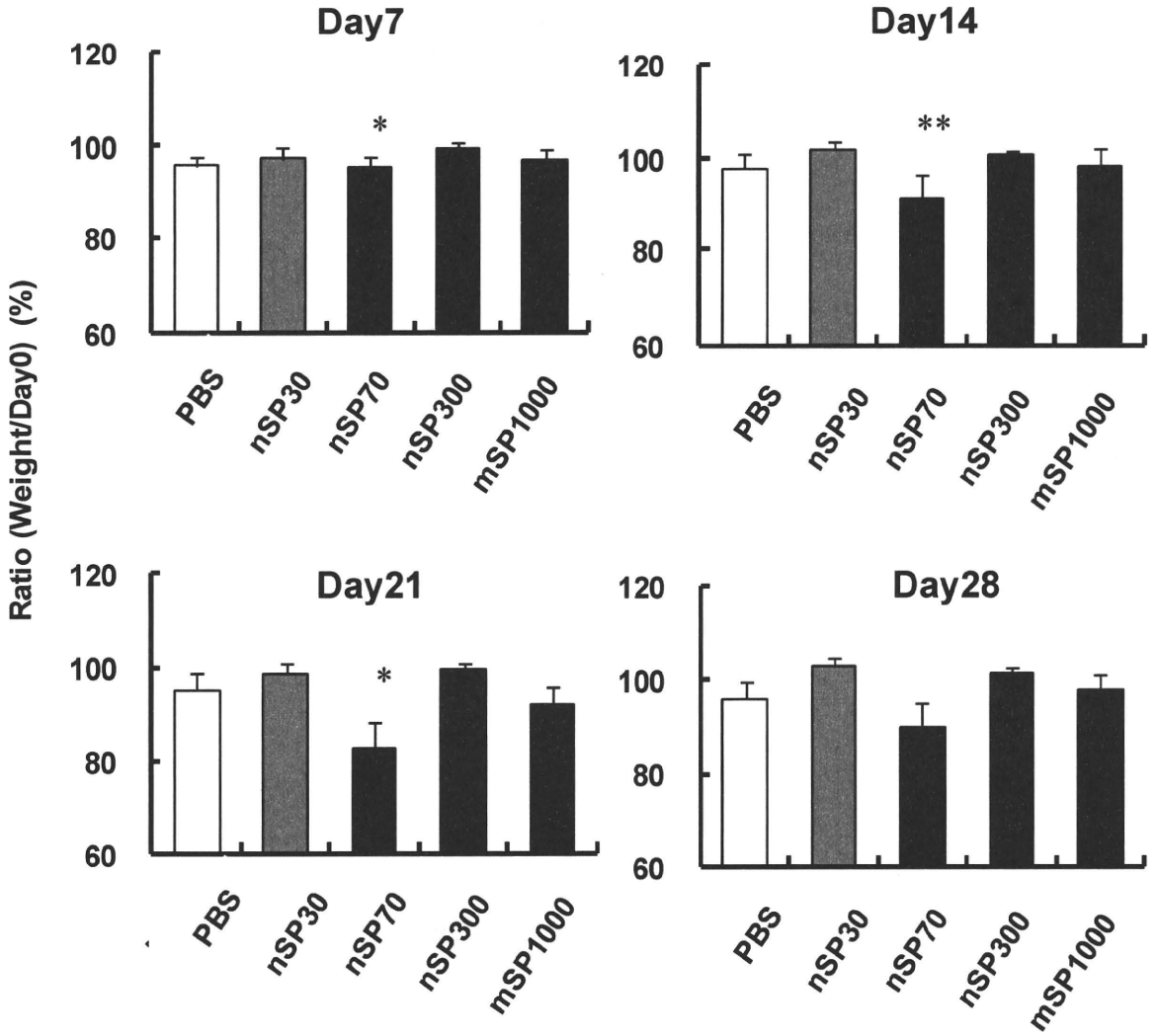

図 8. ナノシリカの経口投与による体重変化の評価

各粒子サイズの非晶質シリカを BALB/C（6 週齢、雌性）に連日経口投与し、経日的に体重を測定した。$^{*}P < 0.05$、$^{**}P < 0.01$ *vs* PBS

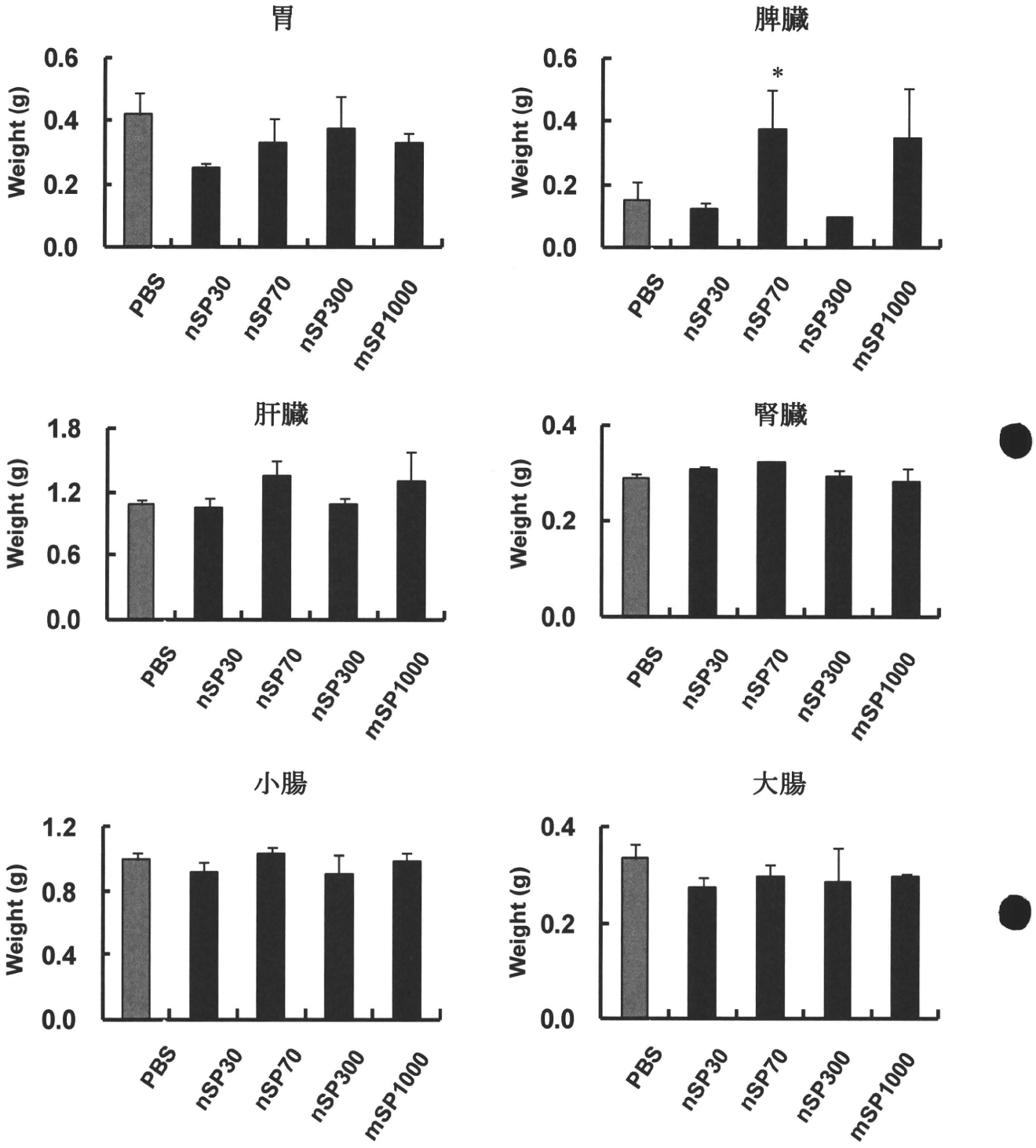

図 9. ナノシリカの経口投与による臓器重量の変化

各粒子サイズの非晶質シリカを BALB/C（6 週齢、雌性）に連日経口投与し、28 日目に臓器を回収し、重量を測定した。$^{*}P < 0.05$ *vs* PBS

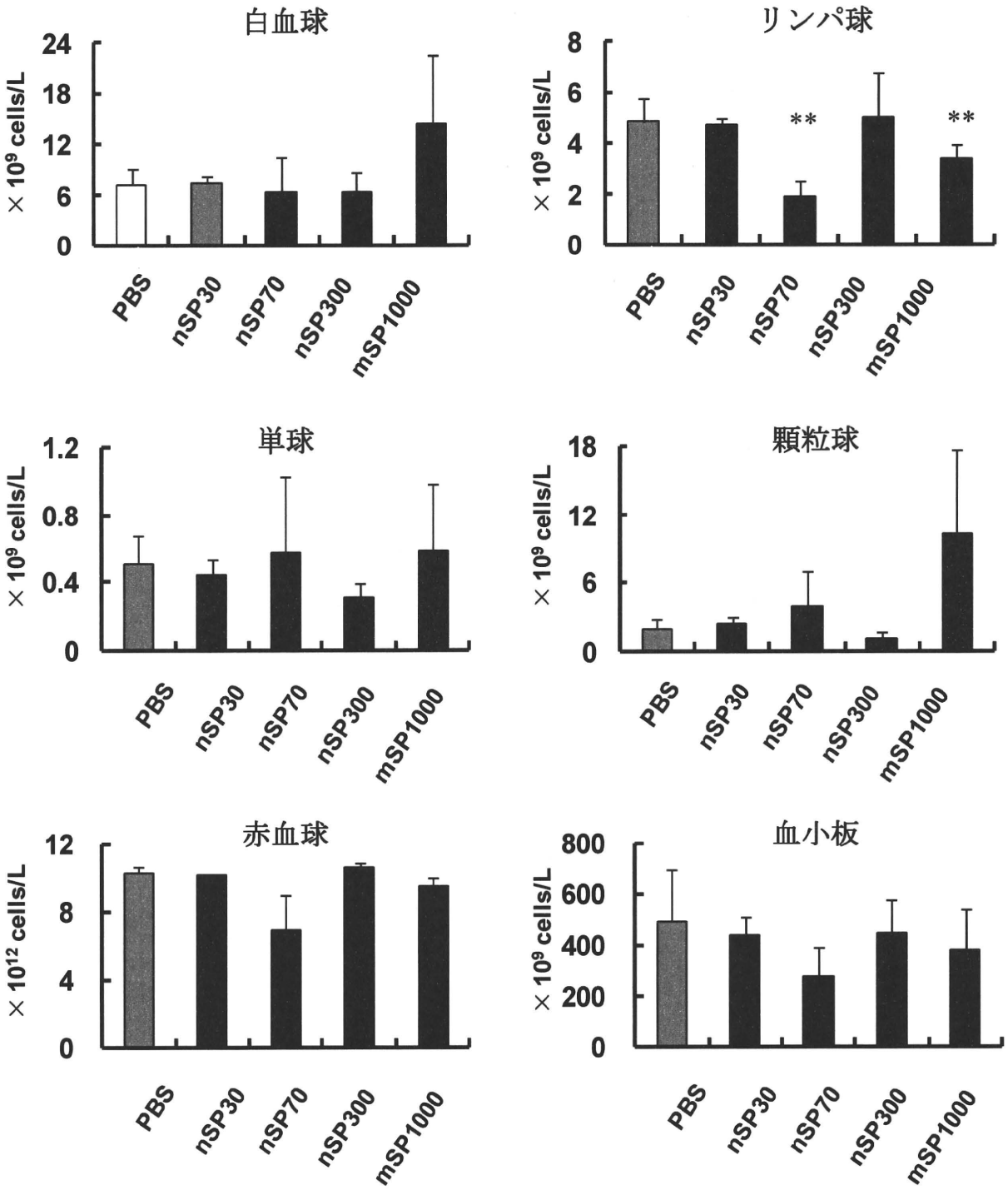

図 10. ナノシリカの経口投与による血球数の変化

各粒子サイズの非晶質シリカを BALB/C（6 週齢、雌性）に連日経口投与し、 28 日目に心臓採血により血球数を測定した。$^{**}P < 0.01$ *vs* PBS

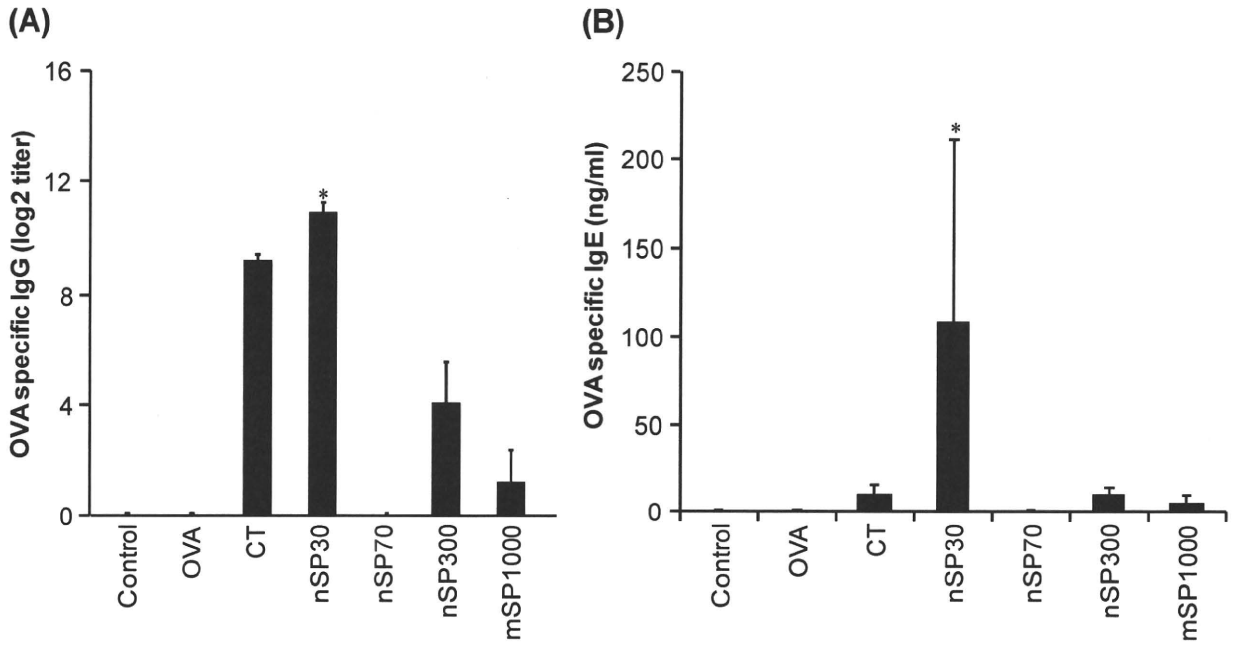

図 11. OVA とシリカを共投与後の OVA 特異的抗体産生評価.

BALB/c マウスに PBS（コントロール）、OVA、OVA とシリカの混合溶液を、1 週間おきに 4 回経口投与した。最終投与 1、2 日後に、再度 OVA を経口投与した。その後、血漿を回収し、OVA 特異的（A）IgG、（B）IgA を ELISA で評価した。$^{*}P < 0.01$ *vs* OVA alone.

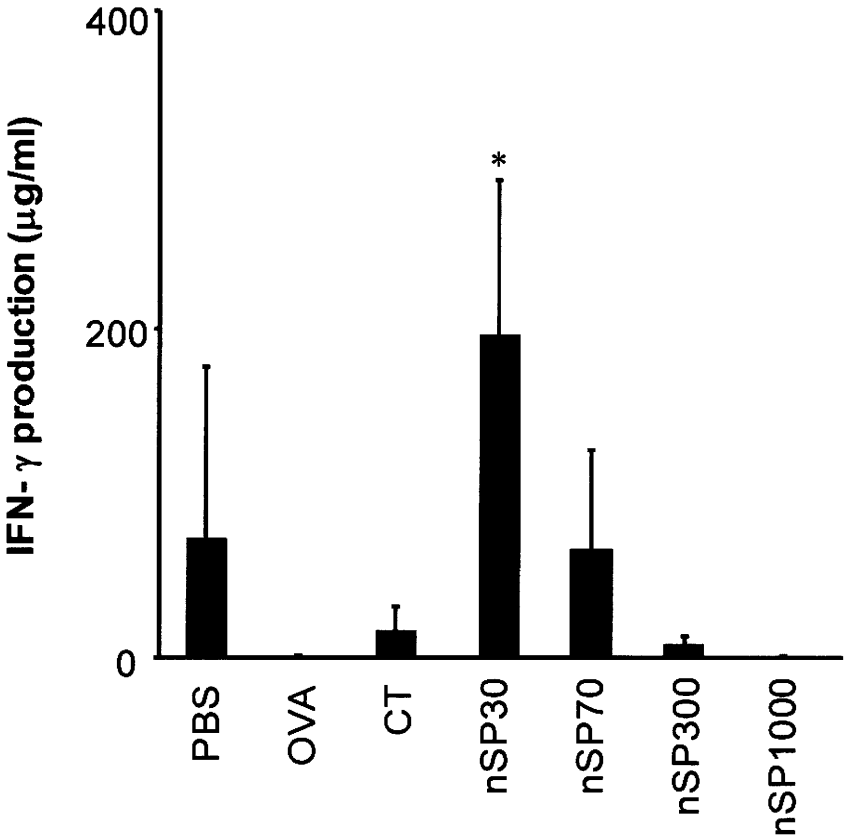

図 12. OVA とシリカを共投与後のサイトカイン産生評価.

図 11 と同様の方法で投与した後、脾臓を回収し、OVA 存在下で 5 日間培養した。その後、培養上清中の IFN-γ 量を ELISA により評価した。*$P < 0.01$ *vs* OVA alone

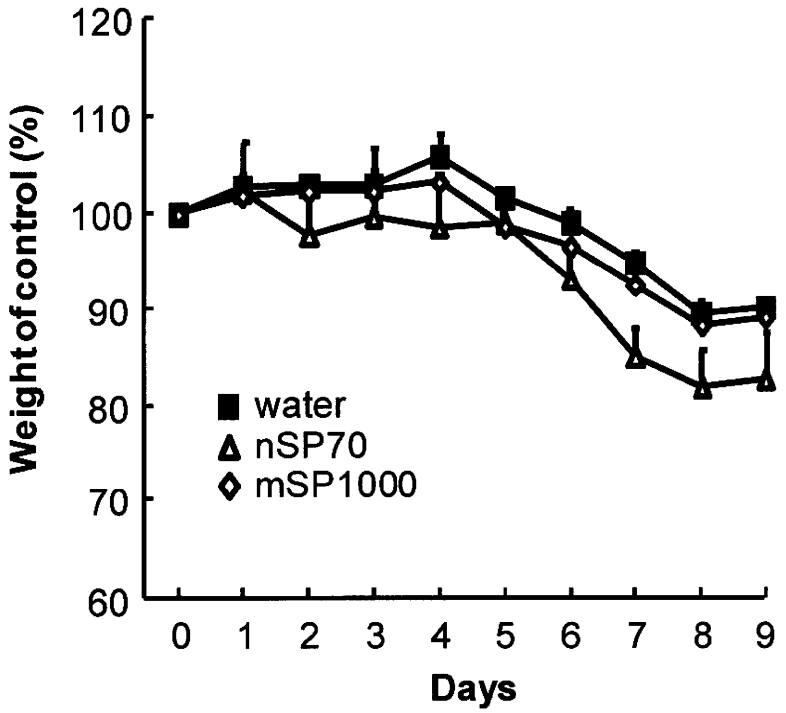

図 13. ナノシリカが **DSS** 誘発性炎症性腸疾患に及ぼす影響評価

マウスに DSS を自由飲水させると同時に、シリカを 1 日 1 回強制経口投与した。その後、経日的に体重を測定した。

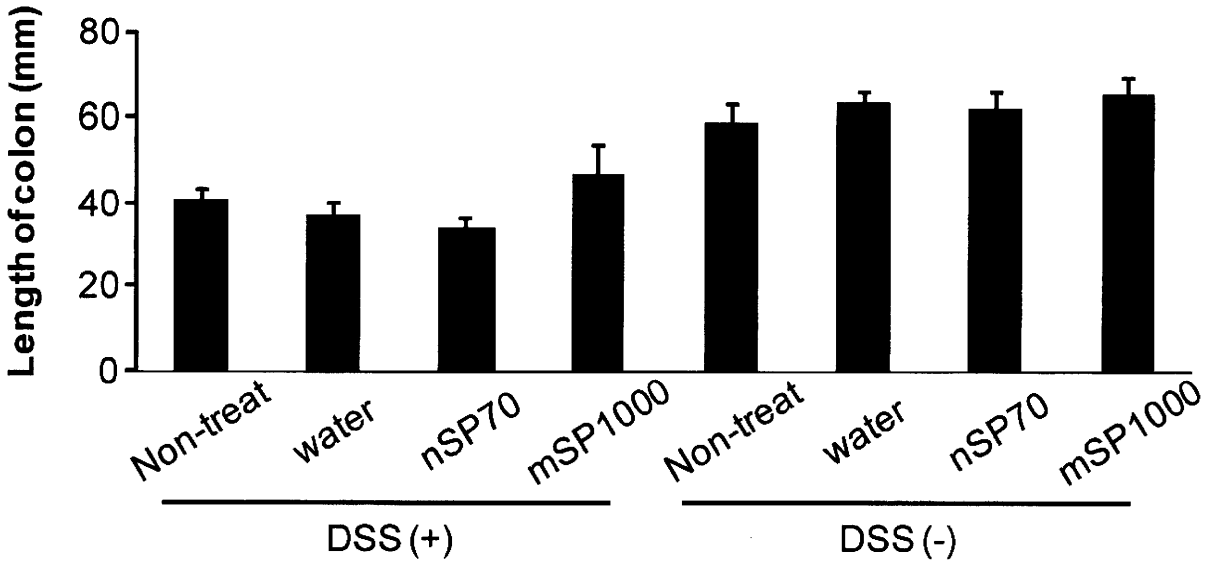

図 14. ナノシリカが DSS 誘発性炎症性腸疾患に及ぼす影響評価

図 13 と同様の方法で投与し、9 日目に解剖し、大腸の長さを測定した。

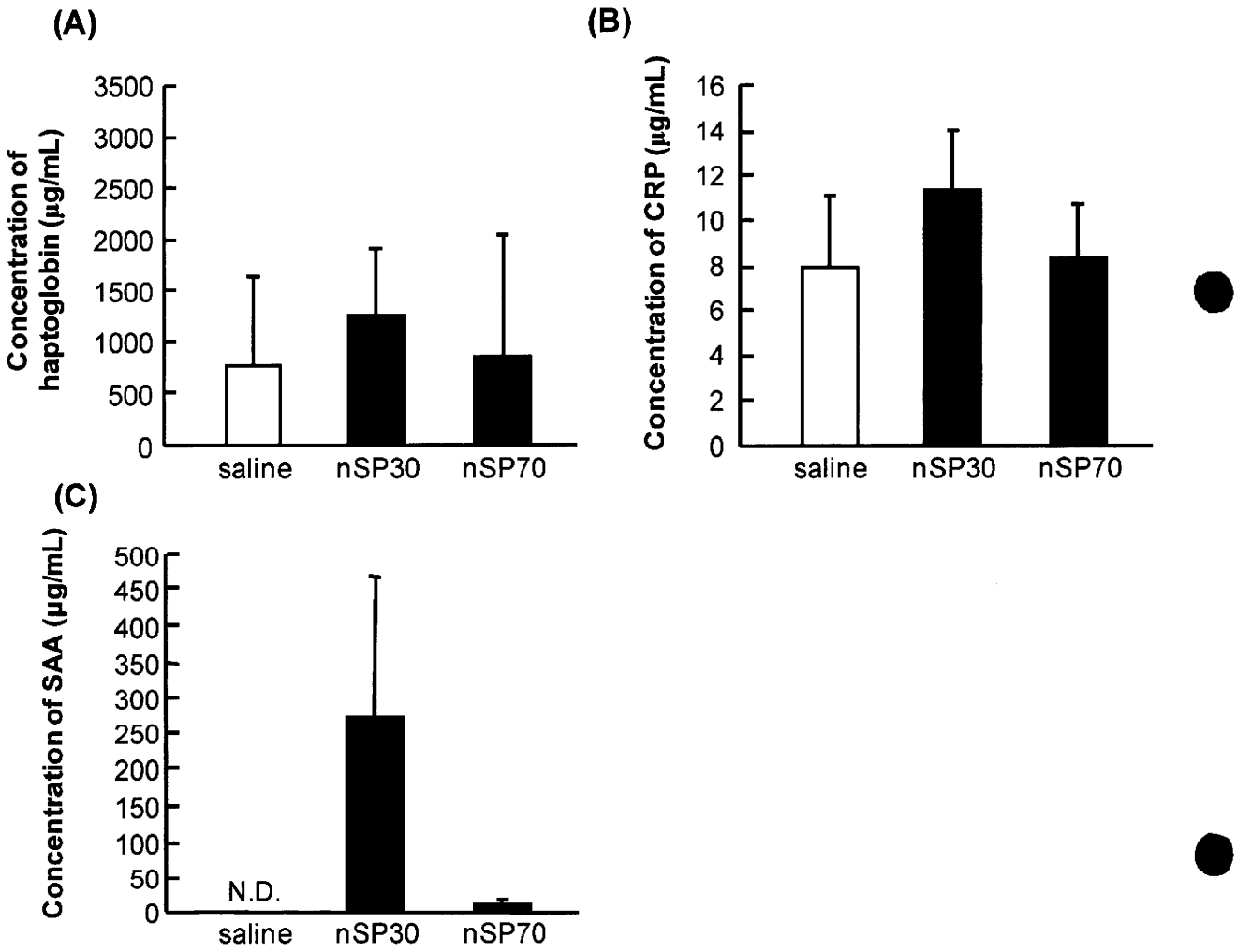

図 15. ナノマテリアルに対する安全性評価マーカーとしての急性期蛋白質の応用

BALB/c に nSP30 もしくは nSP70 を 5 mg/マウスで経口投与した。24 時間後に血漿を回収し、(A) haptoglobin、(B) CRP、(C) SAA を ELISA により評価した。

研究成果の刊行に関する一覧表

雑誌

発表者氏名	論文タイトル名	発表誌名	巻号	ページ	出版年
Morishige T, Yoshioka Y, Tanabe A, Yao X, Tsunoda S, Tsutsumi Y, Mukai Y, Okada N, Nakagawa S.	Titanium dioxide induces different levels of IL-1β production dependent on its particle characteristics through caspase-1 activation mediated by reactive oxygen species and cathepsin B	Biochem Biophys Res Commun	392(2)	160-5	2010
Morishige T, Yoshioka Y, Inakura H, Tanabe A, Yao X, Narimatsu S, Monobe Y, Imazawa T, Tsunoda S, Tsutsumi Y, Mukai Y, Okada N, Nakagawa S.	The effect of surface modification of amorphous silica particles on NLRP3 inflammasome mediated IL-1b production, ROS production and endosomal rupture	Biomaterials	31(26)	6833-6842	2010
Morishige T, Yoshioka Y, Inakura H, Tanabe A, Yao X, Tsunoda S, Tsutsumi Y, Mukai Y, Okada N, Nakagawa S.	Cytotoxicity of amorphous silica particles against macrophage-like THP-1 cells depends on particle-size and surface properties	Pharmazie	65(8)	596-9	2010
Yoshioka Y, Yoshikawa T, Tsutsumi Y.	Nano-safety science for assuring the safety of nanomaterials	Nippon Eiseigaku Zasshi	65(4)	487-92	2010
Higashisaka K, Yoshioka Y, Yamashita K, Morishita Y, Fujimura M, Nabeshi H, Nagano K, Abe Y, Kamada H, Tsunoda S, Yoshikawa T, Itoh N, Tsutsumi Y.	Acute phase proteins as biomarkers for predicting the exposure and toxicity of nanomaterials	Biomaterilas	32(1)	3-9	2011
Nabeshi H, Yoshikawa T, Arimori A, Yoshida T, Tochigi S, Kondoh S, Hirai T, Akase T, Nagano K, Abe Y, Kamada H, Tsunoda S, Itoh N, Yoshioka Y, Tsutsumi Y.	Effect of surface properties of silica nanoparticles on their cytotoxicity and cellular distribution in murine macrophages	Nanoscale Res Lett			In press

Biochemical and Biophysical Research Communications 392 (2010) 160–165

Contents lists available at ScienceDirect

Biochemical and Biophysical Research Communications

journal homepage: www.elsevier.com/locate/ybbrc

Titanium dioxide induces different levels of IL-1β production dependent on its particle characteristics through caspase-1 activation mediated by reactive oxygen species and cathepsin B

Tomohiro Morishige [a,1], Yasuo Yoshioka [a,b,*,1], Aya Tanabe [a,1], Xinglei Yao [a], Shin-ichi Tsunoda [b,c], Yasuo Tsutsumi [b,c,d], Yohei Mukai [a], Naoki Okada [a], Shinsaku Nakagawa [a,b,*]

[a] Laboratory of Biotechnology and Therapeutics, Graduate School of Pharmaceutical Sciences, Osaka University, 1-6 Yamadaoka, Suita, Osaka 565-0871, Japan
[b] The Center for Advanced Medical Engineering and Informatics, Osaka University, 1-6 Yamadaoka, Suita, Osaka 565-0871, Japan
[c] Laboratory of Pharmaceutical Proteomics, National Institute of Biomedical Innovation, 7-6-8 Saito-Asagi, Ibaraki, Osaka 567-0085, Japan
[d] Laboratory of Toxicology and Safety Science, Graduate School of Pharmaceutical Sciences, Osaka University, 1-6 Yamadaoka, Suita, Osaka 565-0871, Japan

ARTICLE INFO

Article history:
Received 22 December 2009
Available online 7 January 2010

Keywords:
Cytokine
Inflammation
Macrophage
NALP3
Nanomaterial

ABSTRACT

Although titanium dioxide (TiO_2) is widely used, its inhalation can induce inflammatory diseases accompanied by interleukin-1β (IL-1β) production. The particle characteristics of TiO_2 are important factors in its biological effects. It is urgently necessary to investigate the relationship between the particle characteristics and biological responses for the development of safe forms of TiO_2. Here, we systematically compared the production of IL-1β in response to various forms of TiO_2 by macrophage-like human THP-1 cells using various sizes (nano to micro), crystal structures (anatase or rutile), and shapes (spherical or spicular) of TiO_2. The production of IL-1β depended dramatically on the characteristics of the TiO_2. Notably, smaller anatase and larger rutile particles provoked higher IL-1β production. In addition, IL-1β production depended on active cathepsin B and reactive oxygen species production independent of the characteristics of TiO_2. Our results provide basic information for the creation of safe and effective novel forms of TiO_2.

Introduction

Titanium dioxide (TiO_2) is a natural mineral that occurs in three different crystallographic structures: rutile, anatase, and brookite. Because of its physicochemical properties of good fatigue strength, machinability, biocompatibility, and whitening and photocatalytic effects, TiO_2 is widely used in paints, wastewater treatment, sterilization, cosmetics, foods, biomedical ceramics, and implanted biomaterials. Rutile is used in pigments and sunscreens. Anatase is used as an efficient photocatalyst and in printing ink. TiO_2 is commercially manufactured in large quantities around the world because it is considered to be of low toxicity [1,2]. However, the increasing use of TiO_2 has raised public concern about the potential risks to human health. For instance, TiO_2 can induce lung inflammation and brain damage [3–9]. It has become evident that particle characteristics, including particle size, surface properties, crystal structure, and physical attributes, are important factors in cellular responses. Therefore, it is necessary to evaluate the association between the particle characteristics of TiO_2 and its biological effects.

Inflammation has been suggested as a key factor in the development of fibrosis and cancers [10]. Studies have shown that TiO_2 induces substantial, albeit transient, inflammation accompanied by significant interleukin-1β (IL-1β) production [6,8]. Macrophages and the IL-1β produced by them have been suggested to play a crucial role during the early inflammatory response after exposure to TiO_2 [6,8]. The pro-inflammatory cytokine IL-1β is involved in the initiation of inflammatory processes and thus contributes to inflammatory diseases [11]. In fact, the IL-1β receptor antagonist anakinra has been successfully used to treat patients suffering from inflammatory diseases, indicating underlying increased IL-1β production [12,13]. Therefore, for the development of safe novel forms of TiO_2, systematic analysis of the association between particle characteristics of TiO_2 and IL-1β production levels and the elucidation of the mechanisms of TiO_2-induced IL-1β production are urgently needed.

Mature IL-1β is produced through the cleavage of inactive pro-IL-1β precursor by caspase-1, which is activated within a large

* Corresponding authors. Addresses: The Center for Advanced Medical Engineering and Informatics, Osaka University, 1-6 Yamadaoka, Suita, Osaka 565-0871, Japan. Fax: +81 6 6879 8177 (Y. Yoshioka); Laboratory of Biotechnology and Therapeutics, Graduate School of Pharmaceutical Sciences, Osaka University, 1-6 Yamadaoka, Suita, Osaka 565-0871, Japan. Fax: +81 6 6879 8179 (S. Nakagawa).
E-mail addresses: yasuo@phs.osaka-u.ac.jp (Y. Yoshioka), nakagawa@phs.osaka-u.ac.jp (S. Nakagawa).
[1] These authors contributed equally to this work.

0006-291X/$ - see front matter © 2010 Elsevier Inc. All rights reserved.
doi:10.1016/j.bbrc.2009.12.178

Table 1
Particle characteristics of TiO_2.

	Crystal form	Size
A-1	Anatase	<50 μm
A-2	Anatase	<25 nm
A-3	Anatase	10 nm
R-1	Rutile	<5 μm
R-2	Rutile	30–40 nm
R-3	Rutile	10 nm × 40 nm (spicula)

multimolecular complex termed the inflammasome [14]. The NACHT domain-, leucine-rich repeat-, and pyrin domain (PYD)-containing protein 3 (NALP3) inflammasome, composed of the cytoplasmic receptor NALP3, the adaptor apoptosis-associated speck-like protein containing a CARD domain (ASC), and caspase-1, is implicated in the production of mature IL-1β in response to diverse stimuli [15]. Although the mechanisms of NALP3 activation remain unclear, two separate groups have recently clarified the mediator of NALP3 activation: Cassel et al. demonstrated that phagocytosis of crystalline silica by macrophages induces reactive oxygen species (ROS) production, which contributes to NALP3 activation [16], and Hornung et al. showed that it induces lysosomal destabilization and subsequent release of cathepsin B into the cytoplasm, leading to NALP3 activation [17]. However, it is unclear whether the TiO_2-induced IL-1β production is similarly dependent on NALP3 activation, and it is unknown whether different forms of TiO_2 induce IL-1β production in common or distinct pathways.

Here, we examined the associations between characteristics of forms of TiO_2 and IL-1β production. In addition, we investigated the IL-1β production mechanisms induced by various forms of TiO_2 on macrophage-like THP-1 cells for the creation of novel safe forms of TiO_2.

Materials and methods

Materials and reagents. We used various forms of TiO_2 with two types of crystal structure, different diameters, and different shapes: anatase (A-1 to A-3) and rutile TiO_2 (R-1 to R-3) (Table 1). A-1 to A-3, R-1, and R-2 are spherical, while R-3 is spicular. A-1, A-2, R-1, and R-3 were purchased from Sigma (St. Louis, MO, USA), and A-3 and R-2 were purchased from NanoAmor (Los Alamos, NM, USA). Phorbol 12-myristate 13-acetate (PMA), cytochalasin D, methyl-β-cyclodextrin (MBCD), butylated hydroxyanisole (BHA), diphenyleneiodonium chloride (DPI), and lipopolysaccharide (LPS) were purchased from Sigma. Bafilomycin A_1 was purchased from Biomol (Plymouth Meeting, PA, USA). CA-074-methyl ester (CA-074-Me) and zYVAD-fmk were purchased from Merck Calbiochem (Darmstadt, Germany).

Cells. THP-1 cells (human acute monocytic leukemia cell line) were obtained from the American Type Culture Collection (Manassas, VA, USA) and cultured in RPMI-1640 medium (Wako Pure Chemical Industries, Osaka, Japan) supplemented with 10% fetal bovine serum, 2 mM L-glutamine, and antibiotics at 37 °C in a humid atmosphere with 5% CO_2.

Cytokine production induced by TiO_2. THP-1 cells (1.5×10^4 cells/well) were seeded in 96-well plates (Nunc, Rochester, NY, USA). Differentiation of monocytic THP-1 cells into macrophages was induced by incubation with PMA (0.5 μM) for 24 h at 37 °C. Differentiated cells were then stimulated with 20, 100, or 500 μg/mL TiO_2 for 24 h in the presence or absence of LPS, a widely known activator of THP-1 cells. The levels of IL-1β and tumor necrosis factor α (TNFα) in culture supernatants were then assessed by a commercial enzyme-linked immunosorbent assay (ELISA) kit (BD Pharmingen, San Diego, CA, USA) according to the manufacturer's instructions. For assay of inhibitors, PMA-primed THP-1 cells were washed and pre-incubated with cytochalasin D (1 or 5 μM), MBCD (10 μM), zYVAD-fmk (5 or 10 μM), bafilomycin A_1 (50 or 250 nM), CA-074-Me (5 or 10 μM), BHA (20 or 100 μM), or DPI (10 μM) for 30 min. Then cells were stimulated with 500 μg/mL TiO_2 or 3 mM ATP (a well-known IL-1β inducer) for 6 h in the presence of each inhibitor.

Phagocytosis of TiO_2 on PMA-primed THP-1 cells. THP-1 cells (1.5×10^4 cells/well) were seeded in 96-well plates and primed with PMA (0.5 μM) for 24 h at 37 °C. Differentiated cells were then

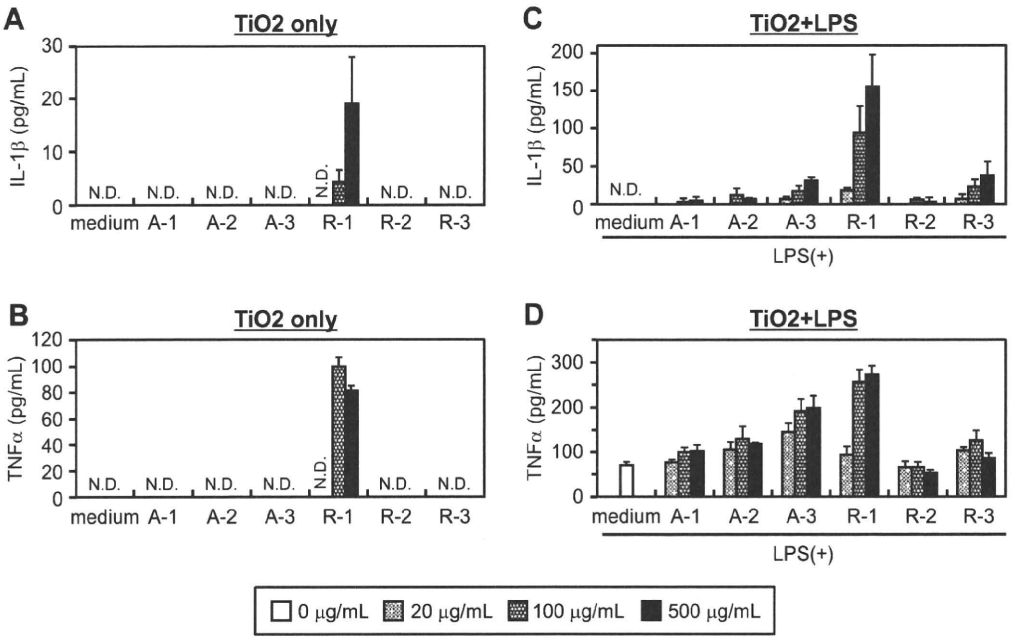

Fig. 1. Association between the characteristics of TiO_2 and cytokine production by THP-1 monocytes. THP-1 monocyte cells were stimulated with 20, 100, or 500 μg/mL of various forms of TiO_2 in the absence (A, B) or presence (C, D) of LPS, and the IL-1β (A, C) or TNFα (B, D) concentrations in the supernatants were evaluated by ELISA. N.D., not detected. Data represent mean ± SD ($n = 4$).

treated with 20 μg/mL TiO_2 for 24 h, and then photographed through a fluorescence microscope (BZ-8000; Keyence Corporation, Osaka, Japan).

Statistical analysis. All results are presented as means ± standard deviation (SD). Differences were compared by Scheffé's method after analysis of variance (ANOVA).

Results and discussion

IL-1β production levels depend on the characteristics of TiO_2

To compare the inflammatory responses, we systematically analyzed the association between characteristics of TiO_2 and levels of IL-1β and TNFα production. We incubated monocytic THP-1 cells with each form of TiO_2 in the absence (Fig. 1A and B) or presence (Fig. 1C and D) of LPS. In the absence of LPS, the larger R-1 induced higher levels of IL-1β and TNFα production than the other forms of TiO_2 (Fig. 1A and B). In the presence of LPS, A-3, and R-3 also induced higher levels of IL-1β production (Fig. 1C). Next we tested PMA-primed macrophage-like THP-1 (THP-1/PMA) cells. Each form of TiO_2 was ingested by THP-1/PMA cells, suggesting that THP-1/PMA cells recognized the TiO_2 as foreign (Fig. 2A). At all concentrations, rutile (especially R-1 and R-3) induced higher IL-1β production than anatase (Fig. 2B). Interestingly, the smallest anatase, A-3, induced higher IL-1β production than the larger A-1 and A-2, whereas the largest rutile, R-1, induced higher IL-1β production than the smaller R-2 and R-3 (Fig. 2B). In addition, spicular R-3 induced higher IL-1β production than the similarly sized and structurally identical but spherical R-2 at the lower concentrations (20 and 100 μg/mL). These results indicate that it is necessary to compare multiple characteristics, including particle size, crystal structure, physical attributes, and surface properties, of TiO_2 to elucidate its biological effects. From these observations, we decided to use A-3, R-1, R-2, and R-3 in further examinations.

Phagocytosis of TiO_2 is an upstream signal in the induction of IL-1β production

Phagocytosis is a key event in initiating macrophage-derived inflammatory responses, and under certain conditions requires lipid raft domains [18,19]. To investigate the association between phagocytosis and TiO_2-induced IL-1β production, we stimulated THP-1/PMA cells with TiO_2 or ATP (control) in the presence of cytochalasin D, a well-characterized inhibitor of phagocytosis that impairs actin-filament assembly. ATP induces IL-1β without cellular internalization and lipid raft formation [20]. Cytochalasin D dramatically abrogated IL-1β production induced by TiO_2, whereas the response to ATP was relatively unaffected (Fig. 3A). Similar results were obtained with MBCD, an inhibitor of lipid raft formation (Fig. 3B). These results indicate that lipid rafts and actin-filament-dependent phagocytosis might be early signals in TiO_2-induced IL-1β production.

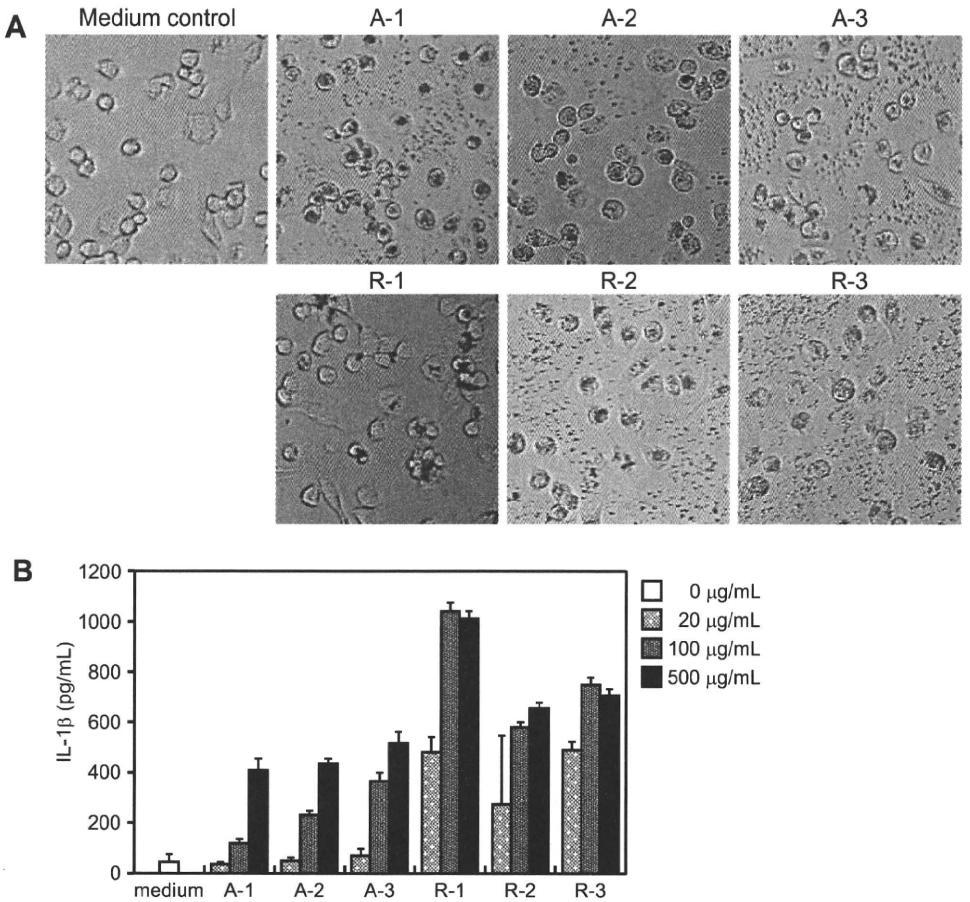

Fig. 2. Association between the characteristics of TiO_2 and cytokine production by differentiated macrophage-like THP-1/PMA cells. (A) THP-1/PMA cells were stimulated with 20 μg/mL of various forms of TiO_2 for 24 h and photographed through a fluorescence microscope. (B) THP-1/PMA cells were stimulated with 20, 100, or 500 μg/mL of various forms of TiO_2 for 6 h, and the IL-1β concentration in the supernatant was evaluated by ELISA. Data represent mean ± SD ($n = 4$; $^{**}P < 0.01$ vs. control).

TiO_2-induced IL-1β production by THP-1/PMA cells depended on caspase-1, ROS, and cathepsin B

Next, we examined how TiO_2 induces IL-1β production. IL-1β is produced from the inactive precursor pro-IL-1β in the cytosol. After cellular activation by a variety of stimuli, the maturation of pro-IL-1β into the mature IL-1β is controlled by caspase-1 [14,21]. To confirm the activation by caspase-1, we treated cells with a caspase-1-specific inhibitor, zYVAD-fmk [22]. zYVAD-fmk completely blocked both ATP- and TiO_2-induced IL-1β production (Fig. 4A), suggesting that the release of IL-1β by TiO_2 is mediated by activated caspase-1.

After assembly of the inflammasome, which activates pro-caspase-1, caspase-1 controls IL-1β maturation. However, how the inflammasome is activated is not well understood. Recently, Hornung et al. reported that crystalline silica induces lysosomal enlargement and loss of lysosomal integrity, leading to the release of the lysosomal contents into the cytoplasm. Furthermore, the release of specific proteases such as cathepsin B seems to be causally related to inflammasome activation [17]. To investigate

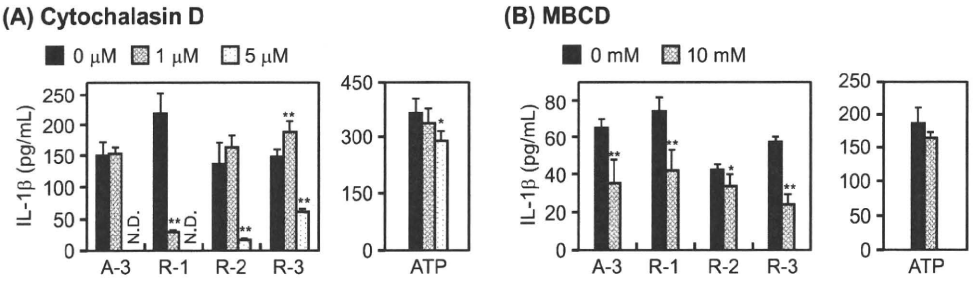

Fig. 3. TiO_2-induced IL-1β production in THP-1/PMA cells is mediated by phagocytosis and lipid rafts. (A, B) IL-1β production levels of THP-1/PMA cells stimulated with 500 μg/mL TiO_2 or 5 mM ATP for 6 h in the presence or absence of (A) cytochalasin D or (B) MBCD at indicated concentrations. IL-1β levels in the culture media were analyzed by ELISA. N.D., not detected. Data represent mean ± SD ($n = 4$; * $P < 0.05$ and ** $P < 0.01$ vs. inhibitor [−]).

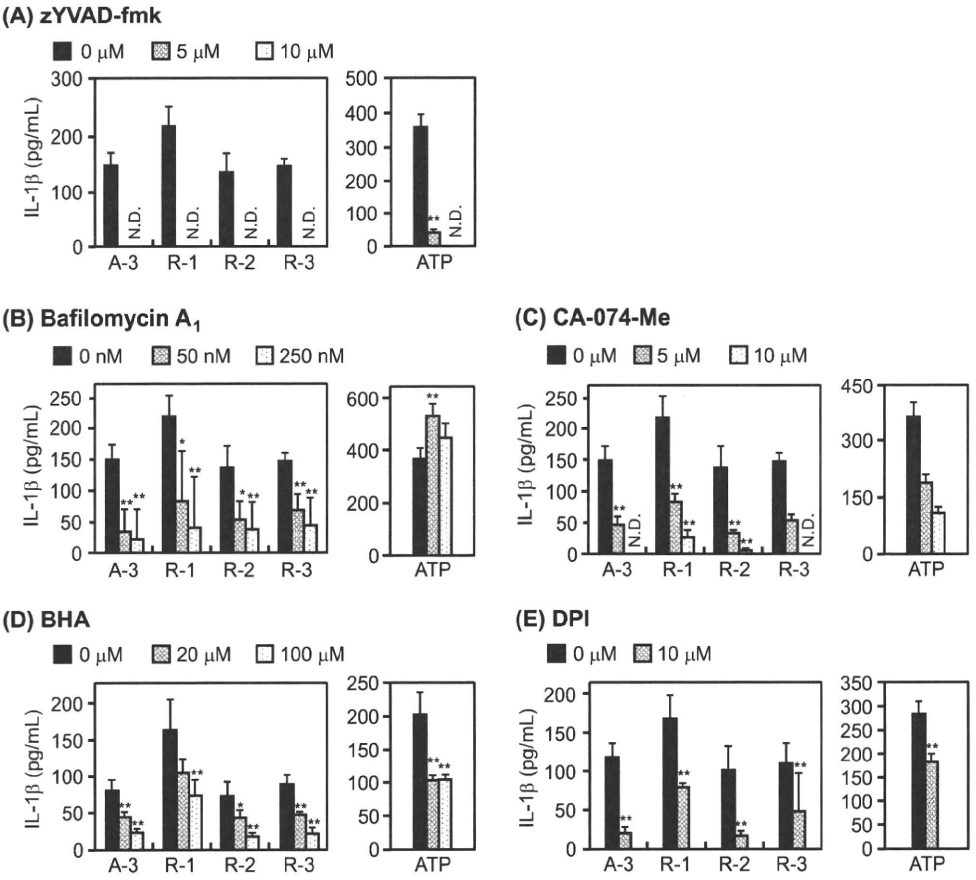

Fig. 4. TiO_2-induced IL-1β production in THP-1/PMA cells is mediated by caspase-1, ROS, and cathepsin B. (A–E) IL-1β production levels of THP-1/PMA cells stimulated with 500 μg/mL TiO_2 or 5 mM ATP for 6 h in the presence or absence of (A) zYVAD-fmk, (B) bafilomycin A_1, (C) CA-074-Me, (D) BHA, or (E) DPI at indicated concentrations. IL-1β levels in the culture media were analyzed by ELISA. N.D., not detected. Data represent mean ± SD ($n = 4$; * $P < 0.05$ and ** $P < 0.01$ vs. inhibitor [−]).

whether cathepsin B mediates TiO_2-induced IL-1β production, we stimulated THP-1/PMA cells with TiO_2 in the presence of a specific inhibitor of the vacuolar H^+-ATPase (bafilomycin A_1) or a membrane-permeable cathepsin B-specific inhibitor (CA-074-Me). Bafilomycin A_1 suppresses the pH decrease in endo-lysosomes; the pH decrease is important for cathepsin B to exert its activity. Both inhibitors almost completely suppressed the IL-1β production induced by TiO_2 independent of the characteristics of TiO_2 (Fig. 4B and C), suggesting that the active cathepsin B is one of the most important common activators of the inflammasome upon TiO_2 stimulation.

It is well known that the stimulation of macrophages with TiO_2 induces ROS production. The inflammasome activator ATP can induce the production of ROS, which are important for caspase-1 activation, suggesting that ROS signaling occurs upstream of inflammasome [16,23,24]. To examine whether ROS are involved in the TiO_2-induced IL-1β production, we stimulated THP-1/PMA cells with TiO_2 in the presence of a broad ROS scavenger, BHA. BHA significantly inhibited the TiO_2-induced IL-1β production (Fig. 4D). We obtained similar results in cells treated with DPI, a specific inhibitor of NADPH-oxidase, an important enzyme in the production of ROS (Fig. 4E) [25]. These results indicate that both cathepsin B and ROS play important roles in TiO_2-induced IL-1β production independent of particle characteristics. We speculate that caspase-1, cathepsin B, and ROS are mutually linked in a single pathway for the TiO_2-induced IL-1β-producing cascade. However, it is unclear how the ROS and cathepsin B interact with each other. Recently, Blomgran et al. showed that ROS production in microbes induces lysosomal rupture, allowing cathepsin B to leak into the cytoplasm [26]. Therefore, we speculate that TiO_2-induced ROS induce lysosomal rupture and subsequent inflammasome/caspase-1 activation. On the other hand, some reports show that after phagocytosis of crystalline silica, the reactive particle surface may interact with the phagolysosomal membranes, leading to lysosomal rupture. This suggests that the surface properties of TiO_2 influence the permeability of the lysosomal membrane [27–29]. We are now examining the association between particle characteristics of TiO_2 and lysosomal responses.

Our results confirm that characteristics of TiO_2 change the activity of posttranscriptional processing of IL-1β mediated by caspase-1. However, for several inflammatory cytokines, including IL-1β, both transcription and posttranslational processing are important for the secretion of their mature forms [17,23,30]. Nuclear factor-κB (NFκB) is a well-known transcription factor that regulates the transcription of various cytokines, including IL-1β and TNFα. Therefore, it is important to investigate the association between characteristics of TiO_2 and NFκB activity for the development of safe forms of TiO_2.

The development of safe and effective nanomaterials is important for technology advancement and for healthy lives. For the creation of such materials, we need more information about the relationship between particle characteristics and biological effects. It has become evident that the surface properties of particles are also very important factors in biological effects [7,9,31]. Therefore, we are now trying to develop a novel method for designing TiO_2 particles, including surface properties, crystal structure, size, and shape, to enable the creation of safe and effective novel materials.

Conclusion

The inflammatory effect of TiO_2 depended dramatically on the particle characteristics. TiO_2-induced IL-1β production was mediated by ROS and cathepsin B independent of the particle characteristics. These results provide important basic information for the development of safe forms of TiO_2.

Conflict of interest

The authors declare that they have no conflicts of interest.

Acknowledgments

This study was supported in part by grants from the Ministry of Education, Culture, Sports, Science and Technology of Japan, and the Ministry of Health, Labor and Welfare in Japan.

References

[1] C.L. Tran, D. Buchanan, R.T. Cullen, et al., Inhalation of poorly soluble particles: II. Influence of particle surface area on inflammation and clearance, Inhal. Toxicol. 12 (2000) 1113–1126.
[2] P.M. Hext, J.A. Tomenson, P. Thompson, Titanium dioxide: inhalation toxicology and epidemiology, Ann. Occup. Hyg. 49 (2005) 461–472.
[3] K.E. Driscoll, J.K. Maurer, Cytokine and growth factor release by alveolar macrophages: potential biomarkers of pulmonary toxicity, Toxicol. Pathol. 19 (1991) 398–405.
[4] E. Bermudez, J.B. Mangum, B.A. Wong, et al., Pulmonary responses of mice, rats, and hamsters to subchronic inhalation of ultrafine titanium dioxide particles, Toxicol. Sci. 77 (2004) 347–357.
[5] E.J. Park, J. Yi, K.H. Chung, et al., Oxidative stress and apoptosis induced by titanium dioxide nanoparticles in cultured BEAS-2B cells, Toxicol. Lett. 180 (2008) 222–229.
[6] J. Wang, Y. Liu, F. Jiao, et al., Time-dependent translocation and potential impairment on central nervous system by intranasally instilled TiO(2) nanoparticles, Toxicology 254 (2008) 82–90.
[7] D. Napierska, L.C. Thomassen, V. Rabolli, et al., Size-dependent cytotoxicity of monodisperse silica nanoparticles in human endothelial cells, Small 5 (2009) 846–853.
[8] E.J. Park, J. Yoon, K. Choi, et al., Induction of chronic inflammation in mice treated with titanium dioxide nanoparticles by intratracheal instillation, Toxicology 260 (2009) 37–46.
[9] K.M. Waters, L.M. Masiello, R.C. Zangar, et al., Macrophage responses to silica nanoparticles are highly conserved across particle sizes, Toxicol. Sci. 107 (2009) 553–569.
[10] B.B. Aggarwal, P. Gehlot, Inflammation and cancer: how friendly is the relationship for cancer patients?, Curr Opin. Pharmacol. 9 (2009) 351–369.
[11] L. Franchi, T. Eigenbrod, R. Munoz-Planillo, et al., The inflammasome: a caspase-1-activation platform that regulates immune responses and disease pathogenesis, Nat. Immunol. 10 (2009) 241–247.
[12] P.F. Piguet, C. Vesin, G.E. Grau, et al., Interleukin 1 receptor antagonist (IL-1ra) prevents or cures pulmonary fibrosis elicited in mice by bleomycin or silica, Cytokine 5 (1993) 57–61.
[13] P.N. Hawkins, H.J. Lachmann, M.F. McDermott, Interleukin-1-receptor antagonist in the Muckle–Wells syndrome, N. Engl. J. Med. 348 (2003) 2583–2584.
[14] L. Agostini, F. Martinon, K. Burns, et al., NALP3 forms an IL-1beta-processing inflammasome with increased activity in Muckle–Wells autoinflammatory disorder, Immunity 20 (2004) 319–325.
[15] A. Halle, V. Hornung, G.C. Petzold, et al., The NALP3 inflammasome is involved in the innate immune response to amyloid-beta, Nat. Immunol. 9 (2008) 857–865.
[16] S.L. Cassel, S.C. Eisenbarth, S.S. Iyer, et al., The Nalp3 inflammasome is essential for the development of silicosis, Proc. Natl. Acad. Sci. USA 105 (2008) 9035–9040.
[17] V. Hornung, F. Bauernfeind, A. Halle, et al., Silica crystals and aluminum salts activate the NALP3 inflammasome through phagosomal destabilization, Nat. Immunol. 9 (2008) 847–856.
[18] M. Kirkham, R.G. Parton, Clathrin-independent endocytosis: new insights into caveolae and non-caveolar lipid raft carriers, Biochim. Biophys. Acta 1745 (2005) 273–286.
[19] M.F. Hanzal-Bayer, J.F. Hancock, Lipid rafts and membrane traffic, FEBS Lett. 581 (2007) 2098–2104.
[20] C.M. Cruz, A. Rinna, H.J. Forman, et al., ATP activates a reactive oxygen species-dependent oxidative stress response and secretion of proinflammatory cytokines in macrophages, J. Biol. Chem. 282 (2007) 2871–2879.
[21] F. Martinon, V. Petrilli, A. Mayor, et al., Gout-associated uric acid crystals activate the NALP3 inflammasome, Nature 440 (2006) 237–241.
[22] S. Mariathasan, D.S. Weiss, K. Newton, et al., Cryopyrin activates the inflammasome in response to toxins and ATP, Nature 440 (2006) 228–232.
[23] C. Dostert, V. Petrilli, R. Van Bruggen, et al., Innate immune activation through Nalp3 inflammasome sensing of asbestos and silica, Science 320 (2008) 674–677.
[24] M.E. Carlotti, E. Ugazio, S. Sapino, et al., Role of particle coating in controlling skin damage photoinduced by titania nanoparticles, Free Radic. Res. 43 (2009) 312–322.
[25] F. Morel, J. Doussiere, P.V. Vignais, The superoxide-generating oxidase of phagocytic cells. Physiological, molecular and pathological aspects, Eur. J. Biochem. 201 (1991) 523–546.

[26] R. Blomgran, L. Zheng, O. Stendahl, Cathepsin-cleaved Bid promotes apoptosis in human neutrophils via oxidative stress-induced lysosomal membrane permeabilization, J. Leukoc. Biol. 81 (2007) 1213–1223.
[27] A.C. Allison, J.S. Harington, M. Birbeck, An examination of the cytotoxic effects of silica on macrophages, J. Exp. Med. 124 (1966) 141–154.
[28] S. Nadler, S. Goldfischer, The intracellular release of lysosomal contents in macrophages that have ingested silica, J. Histochem. Cytochem. 18 (1970) 368–371.
[29] G. Erdogdu, V. Hasirci, An overview of the role of mineral solubility in silicosis and asbestosis, Environ. Res. 78 (1998) 38–42.
[30] S.D. Ha, A. Martins, K. Khazaie, et al., Cathepsin B is involved in the trafficking of TNF-alpha-containing vesicles to the plasma membrane in macrophages, J. Immunol. 181 (2008) 690–697.
[31] X. He, H. Nie, K. Wang, et al., In vivo study of biodistribution and urinary excretion of surface-modified silica nanoparticles, Anal. Chem. 80 (2008) 9597–9603.

Biomaterials 31 (2010) 6833–6842

Contents lists available at ScienceDirect

Biomaterials

journal homepage: www.elsevier.com/locate/biomaterials

The effect of surface modification of amorphous silica particles on NLRP3 inflammasome mediated IL-1β production, ROS production and endosomal rupture

Tomohiro Morishige [a,1], Yasuo Yoshioka [a,b,c,*,1], Hiroshi Inakura [a], Aya Tanabe [a], Xinglei Yao [a], Shogo Narimatsu [a], Youko Monobe [d], Takayoshi Imazawa [d], Shin-ichi Tsunoda [b,c], Yasuo Tsutsumi [b,c,e], Yohei Mukai [a], Naoki Okada [a], Shinsaku Nakagawa [a,b,**]

[a] Laboratory of Biotechnology and Therapeutics, Graduate School of Pharmaceutical Sciences, Osaka University, 1–6 Yamadaoka, Suita, Osaka 565–0871, Japan
[b] The Center for Advanced Medical Engineering and Informatics, Osaka University, 1–6 Yamadaoka, Suita, Osaka 565–0871, Japan
[c] Laboratory of Pharmaceutical Proteomics, National Institute of Biomedical Innovation, 7–6–8 Saito-Asagi, Ibaraki, Osaka 567–0085, Japan
[d] Laboratory of Common Apparatus, Division of Biomedical Research, National Institute of Biomedical Innovation, 7–6–8 Saito-Asagi, Ibaraki, Osaka 567–0085, Japan
[e] Laboratory of Toxicology and Safety Science, Graduate School of Pharmaceutical Sciences, Osaka University, 1–6 Yamadaoka, Suita, Osaka 565–0871, Japan

ARTICLE INFO

Article history:
Received 23 April 2010
Accepted 18 May 2010
Available online 18 June 2010

Keywords:
Cytokine
Inflammation
Interleukin
Macrophage
Nanoparticle
Silica

ABSTRACT

Although amorphous silica particles (SPs) are widely used in cosmetics, foods and medicinal products, it has gradually become evident that SPs can induce substantial inflammation accompanied by interleukin-1β (IL-1β) production. Here, to develop safe forms of SPs, we examined the mechanisms of SP-induced inflammation and the relationship between particle characteristics and biological responses. We compared IL-1β production levels in THP-1 human macrophage like cells in response to unmodified SP of various diameters (30- to 1000-nm) and demonstrated that unmodified microsized 1000-nm SP (mSP1000) induced higher levels of IL-1β production than did smaller unmodified SPs. Furthermore, we found that unmodified mSP1000–induced IL-1β production was depended on the sequence of reactive oxygen species (ROS) production, endosomal rupture, and subsequent activation of pro-inflammatory complex NLRP3 inflammasome. In addition, we compared IL-1β production levels in THP-1 cells treated with mSP1000s modified with a functional group (−COOH, $-NH_2$, $-SO_3H$, −CHO). Although unmodified and surface-modified mSP1000s were taken up with similar frequencies equally into the THP-1 cells, surface modification of mSP1000 dramatically suppressed IL-1β production by reducing ROS production. Our results reveal a part of NLRP3 activation pathway and provide basic information that should help to create safe and effective forms of SPs.

1. Introduction

Amorphous (noncrystalline) silica particles (SPs) possess extraordinary advantages, including straightforward synthesis, relatively low cost, easy separation, and easy surface modification. In addition, SPs are usually considered to have low toxicity, in contrast to crystalline silica, which can cause silicosis and some forms of lung cancer [1,2]. Therefore, SPs have been used for many applications, including in cosmetics, foods, medical diagnosis, cancer therapy, and drug delivery [3–7].

However, the increasing use of SPs has raised public concern about their safety. In fact, current studies have found that SPs induce substantial lung inflammation accompanied by the expression of inflammatory cytokines, including interleukin-1β (IL-1β) [8–10]. Inflammation has been suggested as the key factor in the development of chronic obstructive pulmonary disease (COPD), fibrosis, and carcinogenesis [11–13]. There is therefore an urgent need to investigate the biological inflammatory effects of SPs and ensure their safe use. In addition, it has recently become evident that particle characteristics, including particle size and surface properties, are important factors in pathologic alterations and cellular responses [14–16]. Therefore, for the further development

* Corresponding author at: The Center for Advanced Medical Engineering and Informatics, Osaka University, 1-6 Yamadaoka, Suita, Osaka 565-0871, Japan. Tel./fax: +81 6 6879 8177.
** Corresponding author at: Laboratory of Biotechnology and Therapeutics, Graduate School of Pharmaceutical Sciences, Osaka University, 1-6 Yamadaoka, Suita, Osaka 565-0871, Japan. Tel.: +81 6 6879 8175; fax: +81 6 6879 8179.
E-mail addresses: yasuo@phs.osaka-u.ac.jp (Y. Yoshioka), nakagawa@phs.osaka-u.ac.jp (S. Nakagawa).
[1] Each author contributed equally to the work.

0142-9612/$ – see front matter © 2010 Elsevier Ltd. All rights reserved.
doi:10.1016/j.biomaterials.2010.05.036

of safe SPs, investigation of the mechanisms of SP-induced inflammation and development of a methodology to decrease their inflammatory effects on the basis of evidence of the correlation between particle characteristics and biological effects are very important.

IL-1β is involved in initiation of the inflammatory process and thus contributes to acute and chronic inflammatory diseases. In fact, Cassel et al. reported the possibility that IL-1β induced by inhalation of crystalline silica and asbestos is essential for the development of silicosis and asbestosis, and thus it is needed to investigate whether SPs induce IL-1β production [17–19]. Among the most important sources of IL-1β against inhaled foreign particles are macrophages, which are widely known as the first line of defense [20]. Recently, several studies have shown that the action of macrophage-derived IL-1β is mediated by the activation of a multi-protein complex, called nucleotide-binding oligomerization domain–leucine-rich repeats containing pyrin domain 3 (NLRP3) inflammasome [20]. Production of the cytoplasmic NLRP3 is associated with fever syndromes characterized by spontaneous inflammation [21]. After being activated, NLRP3 interacts with the adaptor molecule apoptosis-associated speck-like protein containing a caspase recruitment domain (ASC) to form a pro-inflammatory complex, NLRP3 inflammasome, which is the principal caspase-1 activator [17,22,23]. Active caspase-1 catalyzes cleavage of the pro-cytokine IL-1β, which is secreted and biologically active only in processed form [23]. Thus, NLRP3 inflammasome is now gaining attention for its role in the initial inflammation generated in response to a number of diverse stimuli [22,24–26]. However, it is unclear whether SPs induce NLRP3 inflammasome activation. Moreover, the mechanisms of activation of NLRP3 inflammasome are poorly understood.

With the aim of developing safe forms of SPs, we evaluated the correlation between inflammatory effect and particle characteristics of SPs of various sizes or with various surface modification groups. Furthermore, we investigated the mechanisms of IL-1β production induced by SPs, concentrating on NLRP3 inflammasome.

2. Materials and methods

2.1. Materials and reagents

Unmodified SPs of diameters between 30 and 1000 nm [nanosized (n)SP30, nSP70, and nSP300, and microsized (m)SP1000], various surface-modified 1000-nm SPs (mSP1000–COOH, $-NH_2$, $-SO_3H$, and –CHO) and FITC-conjugated mSP1000s (unmodified, –COOH, $-NH_2$, $-SO_3H$, and –CHO) were purchased from Micromod Partikeltechnologie (Rostock/Warnemünde, Germany). Phorbol 12-myristate 13-acetate (PMA), cytochalasin D, butylated hydroxyanisole (BHA), and diphenyleneiodonium chloride (DPI) were purchased from Sigma–Aldrich (St. Louis, MO). Bafilomycin A_1 was purchased from Biomol (Plymouth Meeting, PA). CA-074-methyl ester (CA-074-Me), zVAD-fmk, and zYVAD-fmk was purchased from Merck (Darmstadt, Germany).

2.2. Cells and mice

THP-1 (human acute monocytic leukemia cell line) cells were obtained from the American Type Culture Collection (Manassas, VA) and cultured at 37 °C in RPMI (Wako Pure Chemical Industries, Osaka, Japan) supplemented with 10% FBS, 2 mM L-glutamine, and antibiotics. Female C57BL/6 mice were purchased from Nippon SLC (Shizuoka, Japan) and used at 8 weeks of age. All of the animal experimental procedures were performed in accordance with Osaka University's guidelines for the welfare of animals.

2.3. Characterization of silica particle

Size distribution of each SP was measured using a Zetasizer 3000HS (Worcestershire, UK) after sonication with a particle concentration of 300 μg/mL in H_2O.

2.4. Cytotoxicity assay and enzyme-linked immunosorbent assay (ELISA)

THP-1 cells (1.5×10^4 cells/well) were seeded in 96-well plates (Nunc, Rochester, NY) and were then differentiated into macrophages by incubation with 0.5 μM PMA at 37 °C for 24 h followed by one wash with cell culture medium. After the PMA priming, cells were treated with SPs at 100 μg/mL or 3 mM ATP for 6 or 24 h. Cytotoxicity of the SPs was assessed by the standard methylene blue assay method, as previously described [27]. IL-1β production levels in the culture supernatants were assessed with an ELISA kit (BD Pharmingen, San Diego, CA) in accordance with the manufacturer's instructions. For the inhibitory assay, PMA-primed THP-1 cells were pre-incubated for 30 min with cytochalasin D (5 μM), zYVAD-fmk (10 μM), CA-074-Me (2 μM), bafilomycin A_1 (250 nM), BHA (150 μM), DPI (60 μM), or zVAD-fmk (60 μM). The cells were then treated with SPs at 100 μg/mL or with 3 mM ATP for 6 or 24 h.

2.5. In vivo inflammatory effect

C57BL/6 mice were intraperitoneally injected with 1 mg mSP1000s in 200 μL PBS. Six hours after the treatment, the mice were sacrificed and all of the peritoneal cavity lavage fluid (PCLF) was collected in 4 mL PBS. The total number of live cells in the PCLF was determined with a NucleoCounter (Chemometec A/S, Allerød, Denmark).

2.6. Laser scanning confocal microscopy analysis

THP-1 cells (1×10^5 cells/well) were primed with PMA on a Lab-Tek II Chambered Coverglass (Nunc) and incubated for 6 h with 500 μg/mL 10-kDa dextran conjugated with Alexa Fluor 594 (Invitrogen, Carlsbad, CA) and 100 μg/mL mSP1000. The cells were washed and then fixed with 4% paraformaldehyde, and mounted with Prolong Gold Antifade Reagent with DAPI (Invitrogen) for nuclear staining. Fluorescence was observed under a laser scanning confocal microscope (TCS SP2 AOBS; Leica Microsystems, Wetzlar, Germany).

2.7. Transmission electron microscopy (TEM) analysis

THP-1 cells (1×10^5 cells/well) were primed with PMA on a Lab-Tek II Chambered Coverglass and incubated for 6 h with 100 μg/mL mSP1000. They were then fixed in 2.5% glutaraldehyde followed by 1.5% osmium tetraoxide. The fixed cells were dehydrated and embedded in EPON resin. Ultrathin sections were stained with lead citrate and observed by TEM.

2.8. Flow cytometry

THP-1 cells (7×10^5 cells/well) were primed with PMA on 6-well plates and treated with 100 μg/mL mSP1000s for 6 h at 37 °C or 4 °C. After the treatment, cells were detached from the tissue culture plates by incubation with trypsin. Cells were then washed and evaluated in accordance with the Fluorescence-1 (FL-1) parameter using a FACSCalibur flow cytometer (Becton Dickinson, Franklin Lakes, NJ) and Flow Jo software (Three Star, Ashland, OR). Cells were gated to exclude SPs and small cell debris (low forward scatter). Cells with increased FL-1 fluorescence were expressed as a percentage of the maximum number (50,000) of gated cells.

2.9. Reverse transcription polymerase chain reaction (RT-PCR)

THP-1 cells (7×10^5 cells/well) were primed with PMA on 6-well plates and treated with 100 μg/mL mSP1000s for 3 h. After the treatment, total RNA was extracted from the cells by using Sepasol RNA-1 Super (Nacalai Tesque, Kyoto, Japan) in accordance with the manufacturer's instructions. Extracted RNA was reverse-transcribed with SuperScript III (Invitrogen). Synthesized cDNA was amplified by PCR using *Taq* DNA polymerase (Toyobo, Osaka, Japan). The sequences of the specific primers for IL-1β and GAPDH were as follows: IL-1β (F), 5′-AGAAGAACCTATCTTCTTCGA-3′; IL-1β (R), 5′-ACTCTCCAGCTGTAGAGTG G-3′; GAPDH (F), 5′-GCAGGGGGGAGCCAAAAGGG-3′; and GAPDH (R), 5′-TGCCAGCCCCAGCGTCAAAG-3′. After denaturation for 2 min at 95 °C, 20 cycles of three sequential steps—denaturation for 30 s at 95 °C, annealing for 30 s at 60 °C, and extension for 60 s at 72 °C—were performed, ending with a final extension step for 5 min at 72 °C. The PCR products were electrophoresed through a 2% agarose gel, stained with ethidium bromide, and visualized under ultraviolet radiation.

2.10. Observation of activated NLRP3 inflammasome

PMA-primed THP-1 cells were transiently transfected with the plasmid encoding cyan fluorescent protein (CFP)–ASC fusion protein (CFP–ASC) by using ExGen500 *in vitro* transfection agent (Fermentas, Baltimore, MD) in accordance with the manufacturer's instructions [25]. In brief, THP-1 cells (1×10^5 cells/well) were primed with PMA on Lab-Tek II Chambered Coverglass. The cells were then incubated for 60 h in 550 μL of cell culture medium containing the CFP–ASC plasmid (2 μg) – ExGen500 (50 μL) complex. The cells were washed and then treated with 100 μg/mL unmodified mSP1000 for 4 h. After the treatment, the cells were washed and then fixed with 4% paraformaldehyde. They were then mounted with Prolong

Gold Antifade Reagent (Invitrogen). Fluorescence was observed under a confocal laser scanning microscope.

2.11. Evaluation of reactive oxygen species (ROS) production

THP-1 cells (3×10^4 cells/well) were primed with PMA on 96-well black plates (Nunc) and treated with 100 μg/mL mSP1000s for 24 h. The cells were then incubated with 10 μM 2′,7′-dichlorodihydrofluorescein diacetate, acetyl ester (H_2DCFDA; Invitrogen) for 45 min and washed with PBS. Fluorescence was measured at $OD_{485-530}$ using a multi-well spectrophotometer (Molecular Devices, Inc., Tokyo, Japan). ROS production intensity was calculated by using the following formula: ROS production intensity = fluorescence/cell viability. The ROS production intensity of untreated control cells was arbitrarily set to 100%.

2.12. Statistical analysis

All results are presented as means ± SD or SEM. Differences were compared by using Student's *t*-test or Bonferroni's method after ANOVA.

3. Results

3.1. IL-1β production of SPs

To assess the correlation between particle size and the inflammatory effect of SPs, we examined the levels of IL-1β production induced by SPs in THP-1 macrophage-like cells (Fig. 1 A, B). First, we used unmodified SPs of five diameters between 30 and 1000 nm (unmodified nSP30, nSP50, nSP70, and nSP300, and unmodified mSP1000). The mean secondary particle diameters of each SP, measured by Zetasizer, were 33, 44, 79, 326, and 945 nm, respectively (data not shown). We already confirmed that these silica particles were smooth-surfaced spheres and well-dispersing by transmission electron microscopy (data not shown). We incubated THP-1 cells with SPs of each size for 6 h and then analyzed the levels of IL-1β in the culture supernatant. Unmodified mSP1000 induced significantly higher IL-1β production than PBS control, whereas the other, smaller SPs did not induce IL-1β production (Fig. 1A).

Next, to assess the correlation between surface modification and the inflammatory effect of SPs, we used mSP1000s with various surface-modification groups (unmodified, or with an added -COOH, $-NH_2$, $-SO_3H$, or -CHO group) (Fig. 1B). The mean secondary particle diameters of each type of mSP1000 were 945, 1022, 958, 1023, and 969 nm, respectively (data not shown). We incubated THP-1 cells with these surface-modified particles for 6 or 24 h and then examined the IL-1β production levels. Unmodified mSP1000 induced significantly greater IL-1β production than did the medium controls at both 6 and 24 h, whereas the surface-modified mSP1000s induced low levels of IL-1β production (Fig. 1B). The rank order of IL-1β production levels was unmodified mSP1000 > $-$COOH > $-NH_2 = -SO_3H = -$CHO. Furthermore, we evaluated the inflammatory effect of each type of mSP1000 *in vivo*. We intraperitoneally injected mSP1000s into C57CL/6 mice and analyzed the total number of live cells in the PCLF, because inflammation induces local infiltration by various inflammatory cells (Fig. 1C) [28]. The unmodified mSP1000 induced significantly greater cell migration than did the PBS control. The surface-modified mSP1000s did not induce cell accumulation beyond the control level. The rank order of the *in vivo* inflammatory effect was tended to the same as that of IL-1β production *in vitro*. These results indicate that appropriate surface modification with a functional group suppresses the inflammatory effect of unmodified mSP1000.

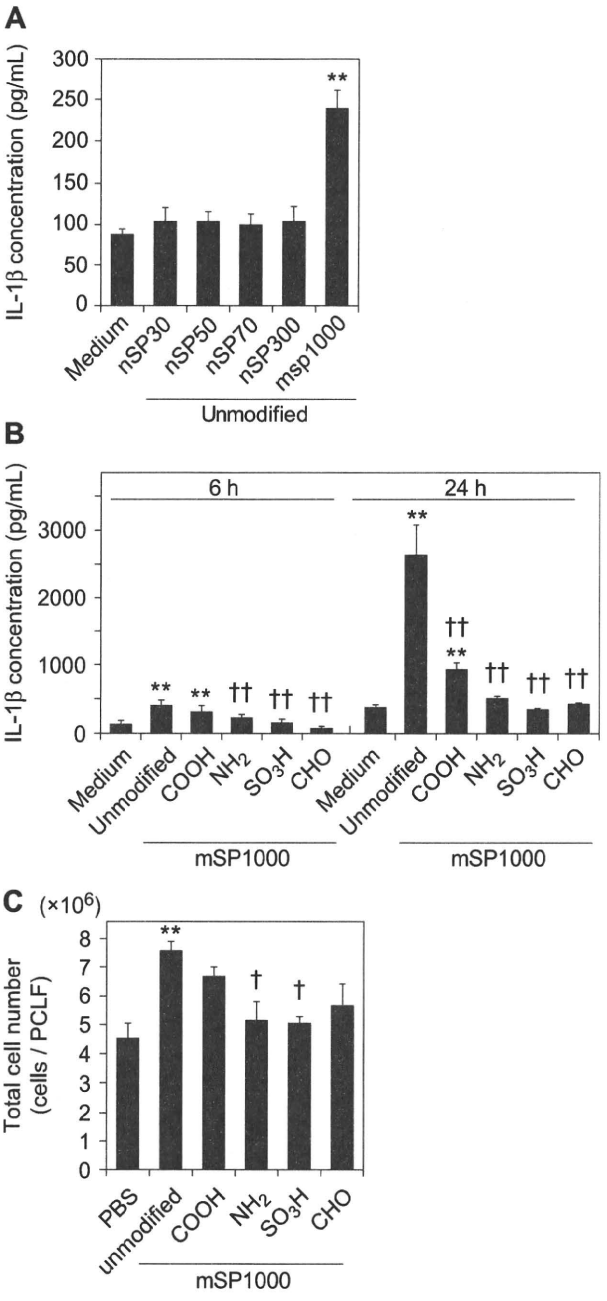

Fig. 1. Correlation between SP characteristics and inflammatory effects *in vitro* and *in vivo*. (A, B) IL-1β production levels in response to SPs of various sizes or with various surface modifications. PMA-primed THP-1 cells were treated with (A) unmodified SPs (30 nm–1000 nm) or (B) unmodified mSP1000, or mSP1000s modified with -COOH, $-NH_2$, $-SO_3H$, or -CHO for 6 or 24 h. IL-1β production levels in the culture supernatant were measured by ELISA. Data represent means ± SD ($n = 5$; $^{**}P < 0.01$ versus value for medium control, $^{\dagger\dagger}P < 0.01$ versus value for unmodified mSP1000, ANOVA). (C) Inflammatory effects of mSP1000s *in vivo*. Mice were intraperitoneally injected with PBS or with 1 mg of one type of mSP1000, and the total numbers of live cells in the PCLF were evaluated after 6 h. Data represent means ± SEM ($n = 5$; $^{*}P < 0.05$ versus value for PBS control, $^{\dagger}P < 0.05$ versus value for unmodified mSP1000, ANOVA).

3.2. Phagocytosis of mSP1000s

Through their phagocytic activity, macrophages play an important role in determining the bio-persistence of foreign particles and initiating inflammatory responses, including IL-1β production [29]. Therefore, to investigate whether mSP1000-induced IL-1β production was triggered by phagocytosis, we pretreated THP-1 cells with cytochalasin D, a well-characterized inhibitor of phagocytosis that impairs actin filament assembly (Fig. 2A). We then

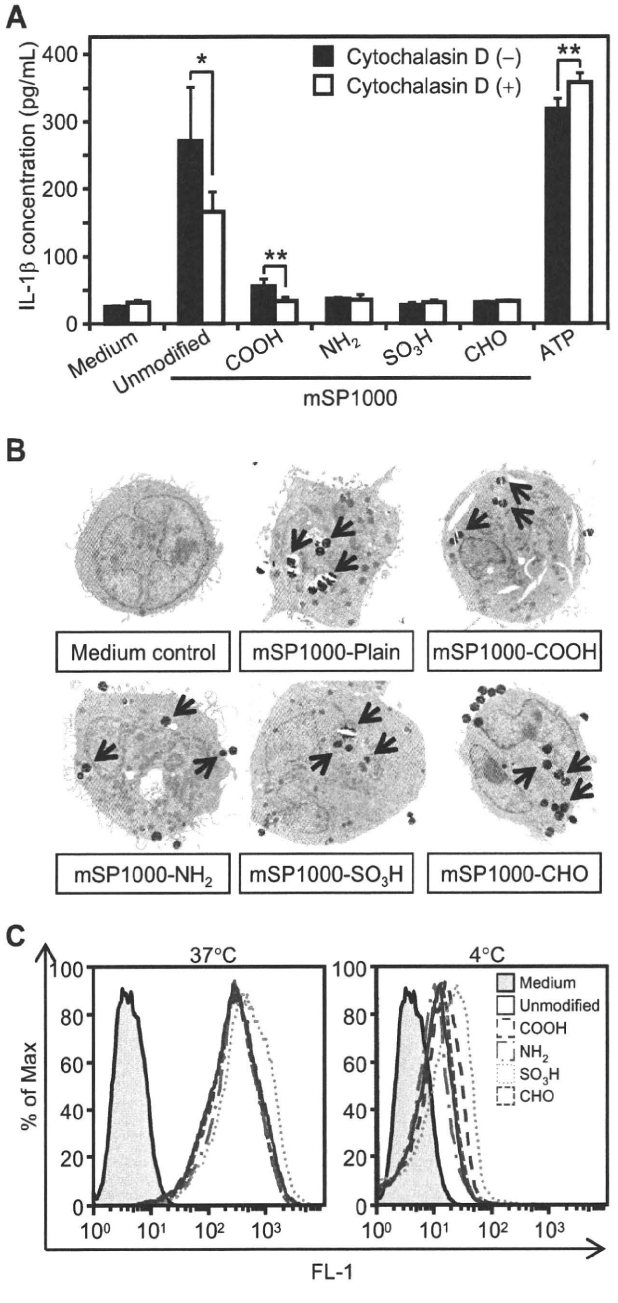

Fig. 2. Phagocytosis is a first signal for mSP1000-induced IL-1β production. (A) Involvement of phagocytosis in mSP1000-induced IL-1β production. PMA-primed THP-1 cells were treated with mSP1000s or ATP for 6 h in the absence (black bars) or presence (white bars) of cytochalasin D (5 μM). IL-1β production levels were then measured by ELISA. Data represent means ± SD ($n = 5$; $^{*}P < 0.05$, $^{**}P < 0.01$ versus value for cytochalasin D [−] control within each treatment pair, t-test). (B) TEM analysis of mSP1000s. PMA-primed THP-1 cells were treated with mSP1000s for 6 h. Cells were then observed by TEM. Arrows indicate ingested mSP1000s. (C) Flow cytometry of FITC-mSP1000s taken up into PMA-primed THP-1 cells. Cells were treated with mSP1000s and incubated for 6 h at 37 °C (left) or 4 °C (right). Data were analyzed by using the FL-1 parameter for green fluorescence.

treated the cells with mSP1000s or ATP, a well-known caspase-1 activator without cellular internalization. The cytochalasin D abolished the mSP1000-induced IL-1β production, whereas the response to ATP was unaffected (Fig. 2A). These results indicate that cellular ingestion of mSP1000s might be the first signal in the inflammatory response. We then speculated that the reduction in IL-1β production through surface modification of mSP1000s resulted from a change in the particle uptake frequency. We used TEM and flow cytometry to evaluate the frequency of uptake of mSP1000s (Fig. 2B, C). TEM analysis clearly showed that both the modified and unmodified mSP1000s were taken up by THP-1 cells (Fig. 2B). Furthermore, flow-cytometric analysis using FITC-conjugated mSP1000s showed that the frequencies of cellular ingestion of modified and unmodified mSP1000s were comparable at 37 °C (Fig. 2C). We also noted that the intensity of FITC-derived fluorescence was almost the same among the different types of mSP1000, and that the increase in the FL-1 signals was dose dependent (data not shown). These results collectively indicate that the unmodified and surface-modified mSP1000s were taken up with similar frequencies equally into the THP-1 cells by actin-dependent phagocytosis, independent of the type of modification group. Therefore, we considered that the difference in IL-1β production levels among mSP1000s was resulted from the signaling intensity in the IL-1β production cascade after ingestion of the mSP1000s by the cell.

3.3. Activation of caspase-1 by mSP1000s

IL-1β production is regulated by pro-IL-1β mRNA expression levels and by caspase-1 activity [17,22,23]. Therefore, to examine the mechanisms of the reduction in IL-1β production by surface modification, we used semi-quantitative RT-PCR to investigate the expression levels of pro-IL-1β mRNA in THP-1 cells treated with each type of mSP1000 (Fig. 3A). There were no significant differences in the expression levels of pro-IL-1β mRNA between cells treated with unmodified and modified mSP1000s. We then tested whether the reduction in IL-1β production by surface modification of mSP1000s resulted from changes in caspase-1 activity induced by mSP1000s. To investigate the association of caspase-1 activity with mSP1000-induced IL-1β production, we treated cells with mSP1000s in the presence of a caspase-1 specific inhibitor, zYVAD-fmk, and analyzed the IL-1β production levels (Fig. 3B). The results showed that zYVAD-fmk almost completely abrogated the IL-1β production induced by mSP1000s. These results collectively indicate that the IL-1β production induced by unmodified mSP1000 depend on the activation of caspase-1. Furthermore, it was speculated that the surface-modified mSP1000s induced little caspase-1 activation.

3.4. Activation of NLRP3 inflammasome by unmodified mSP1000

Recently, NLRP3 inflammasome was identified as the principal activator of caspase-1 in response to several types of danger signal [17,22,23]. To examine whether unmodified mSP1000 exerts their inflammatory potential through NLRP3 inflammasome, we examined the activation of NLRP3 inflammasome on THP-1 cells after treatment with unmodified mSP1000 (Fig. 4) [13,23]. We transiently transfected THP-1 cells with a plasmid expressing CFP–ASC fusion protein. ASC forms large oligomers after its activation, and the clustering of CFP–ASC can be used as an "optical reporter" of the activation of NLRP3 inflammasome [25,30]. Under baseline conditions CFP–ASC fluorescence was evenly distributed in the cytoplasm. Four hours after treatment with unmodified mSP1000, we detected bright fluorescent clusters of CFP–ASC in the cytoplasm. These clusters were not detected in non-transfected THP-1 cells treated with unmodified mSP1000, indicating that the clusters represented cytoplasmic aggregates of activated ASC in NLRP3 inflammasome. These results indicate that mSP1000-induced IL-1β production is mediated by the activation of NLRP3 inflammasome.

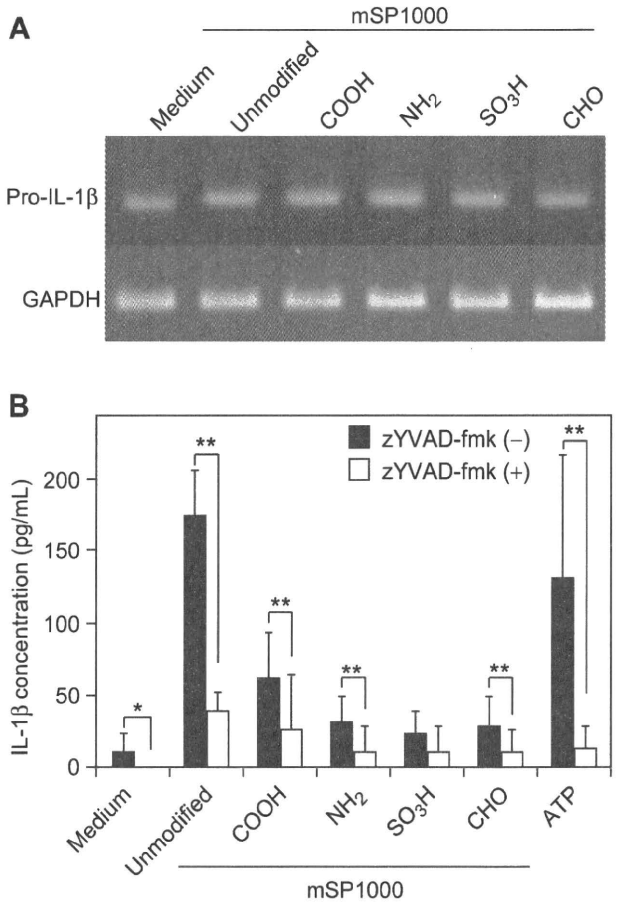

Fig. 3. Differences in levels of IL-1β production induced by each type of mSP1000 depend on caspase-1 activation. (A) Pro-IL-1β mRNA expression levels in mSP1000-treated cells. PMA-primed THP-1 cells were treated with mSP1000s and incubated for 3 h. Then, total RNA was isolated, and RT-PCR was performed with primers specific for IL-1β (top) or GAPDH (bottom). (B) Involvement of caspase-1 activity in mSP1000-induced IL-1β production. PMA-primed THP-1 cells were treated with each type of mSP1000 or with ATP for 6 h in the absence (black bars) or presence (white bars) of zYVAD-fmk (10 μM). IL-1β production levels were analyzed by ELISA. Data represent means ± SD ($n = 5$; $^{*}P < 0.05$, $^{**}P < 0.01$ versus value for zYVAD-fmk [−] control within each treatment pair, *t*-test).

3.5. Endosomal rupture and cathepsin B leakage

With crystalline silica, Hornung et al. reported that endosomal rupture plays a central role in activation of NLRP3 inflammasome followed by leakage of cathepsin B, a endosomal hydrolytic enzyme [20]. To investigate the mechanisms of IL-1β production induced by mSP1000, we compared the frequency of endosomal rupture and subsequent cathepsin B leakage among each type of mSP1000, using Alexa Fluor 594 dextran as an endocytic compartment marker [31]. Mature endosomes incorporating dextran are observed as dotted forms, and the spread of dextran into the cytoplasm is recognized as an indicator of endosomal rupture [20]. We incubated THP-1 cells with dextran and different types of mSP1000 and observed the behavior of the ingested dextran by confocal microscopy (Fig. 5A). Upon treatment of the cells with unmodified mSP1000, we detected the obvious spread of dextran throughout the cytosol, unlike in untreated control cells, indicating that unmodified mSP1000 induced endosomal rupture (Fig. 5A). In contrast, the degree of endosomal rupture was decreased in cells treated with surface-modified mSP1000s, while mSP1000–COOH induced endosomal rupture to some extent as the IL-1β production levels (Fig. 5A). To investigate whether cathepsin B was involved in mSP1000-induced IL-1β production, we treated cells with mSP1000s in the presence of a specific inhibitor of vacuolar H^+-ATPase (bafilomycin A_1), which is needed to activate cathepsin B and a membrane-permeable cathepsin B-specific chemical inhibitor (CA-074-Me). Both inhibitors almost completely suppressed IL-1β production induced by mSP1000s (Fig. 5B and C). These results collectively suggest that the activation of NLRP3 inflammasome and subsequent IL-1β production induced by mSP1000s are triggered by active cathepsin B leakage into the cytoplasm. Furthermore, they suggest that the reduction in IL-1β production by surface modification of mSP1000s results from a reduction in the frequency of mSP1000-induced endosomal rupture and subsequent cathepsin B leakage.

3.6. ROS production of mSP1000s

Another study has shown that ROS, in addition to cathepsin B, plays a crucial role in NLRP3 activation [13,19]. To investigate whether mSP1000-induced activation of NLRP3 inflammasome is dependent on ROS, we measured the levels of ROS in mSP1000-treated THP-1 cells by H_2DCFDA [32]. Treatment of THP-1 cells with unmodified mSP1000, but not with surface-modified SP1000s, significantly enhanced ROS production compared with that in the medium control (Fig. 6A). To confirm the involvement of ROS in mSP1000-induced IL-1β production, we evaluated the levels of IL-1β induced by mSP1000s in the presence of a broad ROS scavenger, BHA, or a specific inhibitor of NADPH oxidase, DPI. NADPH oxidase is an important enzymatic source for the production of ROS [33]. We confirmed that both BHA and DPI significantly suppressed unmodified mSP1000–induced IL-1β production (Fig. 6B and C). These results indicate that, in addition to cathepsin B, mSP1000-induced ROS play an important role in NLRP3 activation.

We then examined the association between mSP1000-induced ROS production and endosomal rupture. We incubated cells with dextran and unmodified mSP1000 in the presence of BHA and observed the behavior of the dextran as a reflection of endosomal morphology. The endosomal rupture induced by unmodified mSP1000 was almost completely suppressed by BHA (Fig. 6D). These observations collectively suggest that ROS production induced by phagocytosis of unmodified mSP1000 triggered endosomal rupture followed by the activation of NLRP3 inflammasome and subsequent IL-1β production. Furthermore, they also strongly indicate that the reduction in ROS production by surface modification attributes to the decrement of the IL-1β production seen with unmodified mSP1000.

3.7. Cell death by unmodified mSP1000

We reported previously that mSP1000-induced cell death is dependent in part on ROS but independent of caspase-1, -3, -4, and -7, and we also showed that surface modification of mSP1000 significantly suppresses particle cytotoxicity [34]. Here, we speculated that mSP1000-induced cell death was dependent on cathepsin B leakage or on IL-1β signaling triggered by ROS production. Therefore, to investigate the association of cathepsin B and IL-1β signaling with mSP1000-induced cell death, we treated THP-1 cells with unmodified mSP1000 in the presence or absence of CA-074-Me, bafilomycin A_1, or zYVAD-fmk. CA-074-Me and bafilomycin A_1, but not zYVAD-fmk, significantly suppressed the cytotoxicity of unmodified mSP1000 (Fig. 6E). These findings indicate that unmodified mSP1000–induced cell death depends in part on ROS and active cathepsin B but is independent of caspases and IL-1β signals.